



University for the Common Good

Quantification of the performance of iterative and non-iterative computational methods of locating partial discharges using RF measurement techniques

El Mountassir, Othmane; Stewart, Brian G.; Reid, Alistair J.; McMeekin, Scott G.

Published in:

Electric Power Systems Research

DOI:

[10.1016/j.epsr.2016.10.036](https://doi.org/10.1016/j.epsr.2016.10.036)

Publication date:

2017

Document Version

Peer reviewed version

[Link to publication in ResearchOnline](#)

Citation for published version (Harvard):

El Mountassir, O, Stewart, BG, Reid, AJ & McMeekin, SG 2017, 'Quantification of the performance of iterative and non-iterative computational methods of locating partial discharges using RF measurement techniques', *Electric Power Systems Research*, vol. 143, pp. 110-120. <https://doi.org/10.1016/j.epsr.2016.10.036>

General rights

Copyright and moral rights for the publications made accessible in the public portal are retained by the authors and/or other copyright owners and it is a condition of accessing publications that users recognise and abide by the legal requirements associated with these rights.

Take down policy

If you believe that this document breaches copyright please view our takedown policy at <https://edshare.gcu.ac.uk/id/eprint/5179> for details of how to contact us.

Quantification of the Performance of Iterative and Non-Iterative Computational Methods of Locating Partial Discharges Using RF Measurement Techniques

Othmane El Mountassir ^{1*}, Brian G Stewart ², Alistair J Reid ³ and Scott G McMeekin ⁴

¹ Offshore Renewable Energy Catapult, 121 George Street, Glasgow G1 1RD, UK

² Department of Electronic and Electrical Engineering, University of Strathclyde, 204 George Street, Glasgow G1 1XW, UK

³ School of Engineering, Cardiff University, The Parade, Cardiff CF24 3AA, UK

⁴ Institute for Sustainable Engineering & Technology, Glasgow Caledonian University, 70 Cowcaddens Road, Glasgow G4 0BA, UK

Abstract

1 Partial discharge (PD) is an electrical discharge phenomenon that occurs when the
2 insulation material of high voltage equipment is subjected to high electric field stress.
3 Its occurrence can be an indication of incipient failure within power equipment such as
4 power transformers, underground transmission cable or switchgear. Radio frequency
5 measurement methods can be used to detect and locate discharge sources by measuring
6 the propagated electromagnetic wave arising as a result of ionic charge acceleration. An
7 array of at least four receiving antennas may be employed to detect any radiated
8 discharge signals, then the three dimensional position of the discharge source can be
9 calculated using different algorithms. These algorithms fall into two categories; iterative
10 or non-iterative.

11 This paper evaluates, through simulation, the location performance of an iterative
12 method (the standard least squares method) and a non-iterative method (the Bancroft
13 algorithm). Simulations were carried out using (i) a “Y” shaped antenna array and (ii) a
14 square shaped antenna array, each consisting of a four-antennas. The results show that
15 PD location accuracy is influenced by the algorithm’s error bound, the number of
16 iterations and the initial values for the iterative algorithms, as well as the antenna
17 arrangement for both the non-iterative and iterative algorithms. Furthermore, this

18 research proposes a novel approach for selecting adequate error bounds and number of
19 iterations using results of the non-iterative method, thus solving some of the iterative
20 method dependencies.

21 **Keywords:** Partial discharges; Iterative algorithms; Non-Iterative algorithms; Radio
22 Frequency; Fault location; Time difference of arrival.

23 **1 Introduction**

24 Radio frequency (RF) measurement technique using receiving antennas can be used to
25 detect the radiated energy from PD sources or any other electrical discharge activities,
26 subsequently facilitating the discharge source triangulation. Using a receiving antenna
27 array, which may be arranged in various forms, the time differences of arrival (TDOA)
28 between received signals on each of the respective antennas allows the 3 dimensional
29 position of the electrical discharge source to be deduced by processing of the TDOA
30 values through iterative or non-iterative location algorithms. The location of partial
31 discharges using emitted RF techniques in HV equipment has been widely investigated
32 [1-5]. Research in this area has been carried out on cables [6-9], gas and air insulated
33 switchgears [10-14] and transformers [15-17]. PD location in cables, and to a degree in
34 gas-insulated substation (GIS), is a two-dimensional problem, while internal localisation
35 within power transformers and localisation in three dimensions in wide-area HV
36 substations requires robust computation algorithms [1].

37 There are two types of computational algorithm which can be used to locate partial
38 discharges in three dimensions; (i) iterative methods and (ii) non-iterative methods. In
39 this study, a non-iterative method was selected due to the large success of these methods
40 in Global Positioning System (GPS) applications such as navigation and location
41 systems. The choice of an iterative method was mainly due their efficiency in solving
42 nonlinear problems involving large number of variables.

43 The iterative methods give an approximate solution to nonlinear equations based on a
44 number of iterations and starting with an initial value, which is improved at each
45 iteration by an error bound until a converged solution is found or until a maximum
46 number of iterations is reached. Taylor expansion and Newton-Raphson techniques are
47 common iterative methods that can be used to solve the equations of nonlinear systems.

48 These methods have been used in different studies to locate PD [1, 18-19]. The study in
49 [18] highlighted that the performance of the Taylor expansion method depends on the
50 accuracy of the initial values and the number of sensors, whereas the study by [1]
51 showed that the Newton-Raphson method successfully locates PD and that the location
52 accuracy depends on the arrangement of antennas. Study [19] also used the Newton-
53 Raphson method to locate PD and found that in some cases the algorithm did not
54 provide a converged solution. It indicated that a solution called the “grid search
55 method” which consists of using a range of values within a grid as initial values to
56 determine a converged solution helped improve accuracy. Despite the fact that these
57 studies highlighted the success of these iterative methods to locate discharges activities
58 within a reasonable margin of error, a limited number of published studies have
59 attempted to evaluate fully the performance of non-iterative and iterative methods in
60 their ability to locate accurately the position of electrical discharge sources.

61 In order to evaluate the performance of iterative and non-iterative algorithms, the
62 present study investigates through simulation the location performance of a well-
63 established iterative method; the standard least squares (SLS) method, and a non-
64 iterative method; the Bancroft algorithm [22]. Two antenna array configurations (Y and
65 square shape), both consisting of 4 antenna positions were chosen for the investigations
66 reported herein evaluating the performance of the respective location algorithms. The
67 square and ‘Y’ array configurations are commonly used and were selected since they
68 have been used in previous studies [1, 4] to investigate electromagnetic (EM) wave
69 propagation PD sources.

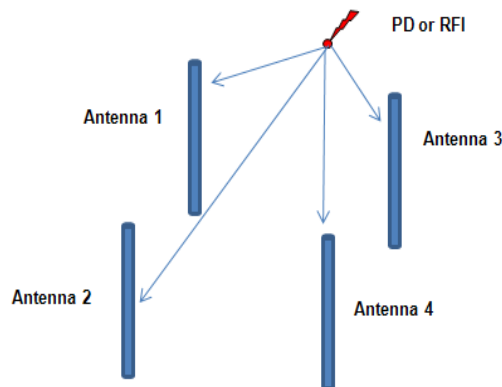
70 The paper is structured as follows: The mathematical formulation of the SLS and
71 Bancroft location algorithms are presented in Section II; Section III presents the
72 methodologies used in the present study; Section IV presents the results of PD location

73 studies using the SLS and Bancroft algorithms respectively (in each case two different
74 antenna arrangements were investigated). For simplification, the simulated PD location
75 data points refer to any electrical discharge source emitting EM wave radiation; Section
76 V compares the characteristics of both the iterative and non-iterative algorithms used;
77 Section VI proposes a new approach to select adequate error bounds and number of
78 iterations using results of the non-iterative methods; Section VII summarises the
79 findings of the study.

80 2 Formulation of the SLS and Bancroft Algorithms

81 A minimum of four spatially separated antennas may be used to triangulate the location
82 of a PD event in 3 dimensions using RF methods (Figure 1). Knowing the grid
83 coordinates of each antenna in the array then allows the propagation time from the PD
84 source to the respective antennas to be calculated using the basic formula $D = v \cdot t$,
85 Where D is distance, v is propagation velocity and t is propagation time. This technique,
86 commonly referred to as ‘triangulation’, is described by Equation (1):

$$87 \quad (x - x_i)^2 + (y - y_i)^2 + (z - z_i)^2 = (v_e \cdot t_i)^2 \quad (1)$$



88 Figure 1: Basic configuration of a typical RF PD location setup.

89 Where (x_i, y_i, z_i) are the coordinates of the i^{th} antenna in Cartesian space, (x, y, z)
90 represent the true coordinates of the PD event, v_e is the speed of light (3×10^8 m/s) and t_i

91 represents the ‘time-of-flight’ of the propagating PD signal from its source to the i^{th}
 92 antenna. It should be noted that since the study is a simulation based investigation, the
 93 speed of light was considered to be in a vacuum and that this value changes depending
 94 on the insulating material.

95 Let the time-of-flight from the PD source to antenna A_1 be T and the time-difference-of-
 96 arrival between antennas A_1 and A_n ($n = 2, 3, 4$) be τ_{1n} . Equation (1) now expands into
 97 the following four formulae [20]:

$$\begin{aligned}
 98 \quad & (x-x_1)^2 + (y-y_1)^2 + (z-z_1)^2 = (v_e \cdot T)^2 \\
 99 \quad & (x-x_2)^2 + (y-y_2)^2 + (z-z_2)^2 = (v_e \cdot (T + \tau_{12}))^2 \\
 100 \quad & (x-x_3)^2 + (y-y_3)^2 + (z-z_3)^2 = (v_e \cdot (T + \tau_{13}))^2 \\
 101 \quad & (x-x_4)^2 + (y-y_4)^2 + (z-z_4)^2 = (v_e \cdot (T + \tau_{14}))^2 \tag{2}
 \end{aligned}$$

102 2.1 Standard Least Squares (SLS) algorithm

103 Using on the non-linear equations in (2), the position of a PD source (x, y, z) can be
 104 computed using the least squares method given in Equation (3).

$$105 \quad S(X) = \sum_{i=1}^N (Y_i(X))^2 \tag{3}$$

106 In least squares, the standard definition of $Y_i(X)$ is given in Equation (4). Based on the
 107 definition of $Y_i(X)$, the least squares method minimises the sum of the square of the
 108 residuals.

$$109 \quad Y_i(X) = \sqrt{(x-x_i)^2 + (y-y_i)^2 + (z-z_i)^2} - (v_e \cdot (T + \tau_{1i})) \tag{4}$$

110 Since the aim is to compute the values of x, y and z which minimise $S(X)$, the partial
 111 derivative of $S(X)$ with respect to x, y and z is calculated with the equation set equal to 0
 112 as shown in Equation (5):

$$113 \quad \frac{\partial S}{\partial x} = 0, \quad \frac{\partial S}{\partial y} = 0, \quad \frac{\partial S}{\partial z} = 0 \quad \text{and} \quad \frac{\partial S}{\partial T} = 0. \tag{5}$$

114 Substituting p to represent x , y or z , the iterative solution for each coordinate and for T
 115 becomes:

$$116 \quad p = \frac{1}{N} \sum_{i=1}^N p_i + \frac{1}{N} \sum_{i=1}^N \frac{(p - p_i)(T + \tau_{1i})v_e}{\sqrt{(x - x_i)^2 + (y - y_i)^2 + (z - z_i)^2}} \quad (6)$$

$$117 \quad T = \frac{\sum_{i=1}^N \sqrt{(x - x_i)^2 + (y - y_i)^2 + (z - z_i)^2}}{\sum_{i=1}^N v_e} - \frac{1}{N} \sum_{i=1}^N \tau_{1i} \quad (7)$$

118 Where N is the number of antennae and τ_{1i} is the TDOA between a signal measured by
 119 the i^{th} antenna and by antenna 1. For chosen initial conditions, the formulae derived
 120 above may be applied iteratively until solutions for x , y and z are converged upon, given
 121 a defined error bound and an upper limit on the number of iterations [4, 21].

122 2.2 Bancroft algorithm

123 Developed by Bancroft [22], this algorithm was derived for application to global
 124 positioning system (GPS) location. Bancroft's algorithm makes use of the Lorenz inner
 125 product for time-space vectors, which is defined considering u and w vectors of the
 126 form:

$$127 \quad \mathbf{u} = \begin{bmatrix} x_u \\ y_u \\ z_u \\ v^* t_u \end{bmatrix}, \quad \mathbf{w} = \begin{bmatrix} x_w \\ y_w \\ z_w \\ v^* t_w \end{bmatrix} \quad (8)$$

128 Where x , y and z are the coordinates of the two vectors u and w , v is a constant which
 129 represent the speed of light, and t is time. The Lorenz inner product of u and w is
 130 defined as:

$$131 \quad \langle \mathbf{u}, \mathbf{w} \rangle = x_u x_w + y_u y_w + z_u z_w - v^2 t_u t_w \quad (9)$$

132 Assuming there are four antennas located at (x_i, y_i, z_i) , with the associated time of arrival
 133 (TOA) as t_i , where $i = 1, 2, 3, 4$ and the PD source is located at (x, y, z) and has a time
 134 of emission (TOE) t . This can be presented as:

$$135 \quad s_i = \begin{bmatrix} x_i \\ y_i \\ z_i \\ v * t_i \end{bmatrix}, \quad s = \begin{bmatrix} x \\ y \\ z \\ v * t \end{bmatrix} \quad (10)$$

136 Each TOA measurement may be expressed as:

$$137 \quad (x - x_i)^2 + (y - y_i)^2 + (z - z_i)^2 = v^2 * (t - t_i)^2 \quad (11)$$

138 Which is equivalent to:

$$139 \quad 2(xx_i + yy_i + zz_i - v^2 t_i t) = x^2 + y^2 + z^2 - v^2 t^2 + x_i^2 + y_i^2 + z_i^2 - v^2 t_i^2 \quad (12)$$

140 or, in vector-matrix form:

$$141 \quad 2As = \lambda I + b \quad (13)$$

142 Where

$$143 \quad s = \begin{bmatrix} x \\ y \\ z \\ v * t \end{bmatrix}, \text{ are the coordinates of interest}$$

$$144 \quad A = \begin{bmatrix} x_1 & y_1 & z_1 & -vt_1 \\ x_2 & y_2 & z_2 & -vt_2 \\ x_3 & y_3 & z_3 & -vt_3 \\ x_4 & y_4 & z_4 & -vt_4 \end{bmatrix}, \quad \lambda = \langle s, s \rangle = x^2 + y^2 + z^2 - v^2 t^2 \quad \text{and} \quad I = \begin{bmatrix} 1 \\ 1 \\ 1 \\ 1 \end{bmatrix}$$

$$145 \quad b = \begin{bmatrix} \langle s_1, s_1 \rangle \\ \langle s_2, s_2 \rangle \\ \langle s_3, s_3 \rangle \\ \langle s_4, s_4 \rangle \end{bmatrix} = \begin{bmatrix} x_1^2 + y_1^2 + z_1^2 - v^2 t_1^2 \\ x_2^2 + y_2^2 + z_2^2 - v^2 t_2^2 \\ x_3^2 + y_3^2 + z_3^2 - v^2 t_3^2 \\ x_4^2 + y_4^2 + z_4^2 - v^2 t_4^2 \end{bmatrix}$$

146 Based on equation (13), which relates s to its Lorentzian norm λ , this can be rewritten as:

$$147 \quad s = \frac{1}{2} \lambda A^{-1} I + \frac{1}{2} A^{-1} b \quad \text{or} \quad s = \lambda d + e \quad (14)$$

148 Where

$$149 \quad d = \frac{1}{2}A^{-1}l = [x_d \quad y_d \quad z_d \quad vt_d]^T, \quad e = \frac{1}{2}A^{-1}b = [x_e \quad y_e \quad z_e \quad vt_e]^T$$

150 Taking the Lorentzian norm of both sides of equation (14) results in a quadratic equation
151 in λ , i.e.

$$152 \quad \lambda = \langle d, d \rangle \lambda^2 + 2\langle d, e \rangle \lambda + \langle e, e \rangle \quad \text{or} \quad \alpha \lambda^2 + \beta \lambda + \gamma = 0 \quad (15)$$

153 Where

$$154 \quad \alpha = \langle d, d \rangle = x_d^2 + y_d^2 + z_d^2 - v^2 t_d^2$$

$$155 \quad \beta = 2\langle d, e \rangle - 1 = 2x_d x_e + 2y_d y_e + 2z_d z_e - 2vt_d t_e - 1$$

$$156 \quad \gamma = \langle e, e \rangle = x_e^2 + y_e^2 + z_e^2 - v^2 t_e^2$$

157 Solving the quadratic equation (15) results in two solutions of λ when
158 $\alpha \neq 0$ and the possible PD solutions are located either at:

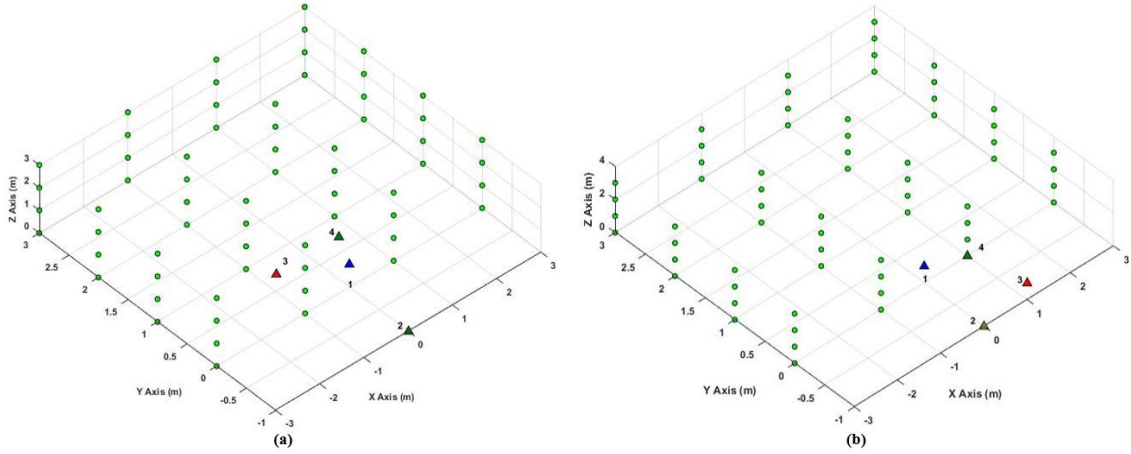
$$159 \quad s_1 = \lambda_1 d + e = \begin{bmatrix} x \\ y \\ z \\ vt \end{bmatrix}, \quad \text{or} \quad s_2 = \lambda_2 d + e = \begin{bmatrix} x \\ y \\ z \\ vt \end{bmatrix} \quad (16)$$

160 In GPS technology, the selection of a valid solution is based on clock synchronisation
161 and thus the solution with the lowest time offset (presented by vt in both s_1 and s_2
162 vector) is considered to be a correct solution.

163 **3 Methodology**

164 The authors have developed a software platform in MATLAB that performs simulation
165 and localisation for an array of PD source positions (a grid of 64 PD positions were
166 simulated, as depicted in Figure 2). The positions were selected arbitrarily on a
167 Cartesian grid as PD sources can occur anywhere within the insulation system of HV
168 assets. Figure 2 also shows the configuration of the antenna arrays (triangular symbols).
169 Simulations have been performed on both the Y shaped (Figure 2a) and the square

170 shaped array (Figure 2b). Table 1 presents the grid coordinates of each antenna. These
 171 antenna arrangement arrays were considered in a way to enable an easy setting of these
 172 equipment when measurements are carried out in a real site environment, although
 173 antenna arrays will generally be placed away from substation equipment to respect
 174 distance clearances.



175
 176 Figure 2: Simulation geometry showing PD locations (green spheres) and antenna locations (triangles) for
 177 the two array configurations (a) Y shaped array and (b) Square shaped array

Table 1: Coordinates of the antenna arrays within the simulation grid

Antenna number	<i>Y shaped array</i>			<i>Square shaped array</i>		
	<i>x (m)</i>	<i>y (m)</i>	<i>z (m)</i>	<i>x (m)</i>	<i>y (m)</i>	<i>z (m)</i>
1	0	0	1	0	0	1
2	0	-1	0	0	-1	0
3	$-1/\sqrt{2}$	$1/\sqrt{2}$	0	1	-1	1
4	$1/\sqrt{2}$	$1/\sqrt{2}$	0	1	0	0

178 In the case of the Y shaped array, the respective antennae were mutually separated by a
 179 distance of 1 m, with 3 of the antennas positioned on the horizontal plane and a single
 180 central antenna elevated by 1m in the vertical plane. In the case of the square array,
 181 antenna positions were spaced apart by 1m horizontally. Diametrically opposite
 182 antennas were offset by 1 m in the z axis. The number of 3D PD locations was chosen
 183 based on processing time considerations. Simulated PD locations fill a defined volume

184 that surrounds the antenna arrays. PD positions lie along the x -axis from 3 m to 3 m at
185 intervals of 2 m, along the y -axis from 0 m to 3 m at intervals of 1 m and along the z -
186 axis from 0 m to 3 m also at intervals of 1 m. The range of the simulated PD positions
187 was selected so that precise appreciation of the location performance of the iterative and
188 non-iterative algorithms was provided.

189 The TDOAs of the simulated PD positions were obtained using Equation 8, where $(x, y,$
190 $z)$ represent the coordinates of the simulated PD position and (x_i, y_i, z_i) the coordinates
191 of the four antennas ($1, 2, 3$ and 4). The iterative algorithm (SLS) was applied and its
192 performance evaluated, with the initial values for (x, y, z) set to $(0, 0, 0)$. Within the
193 iteration method, error bounds were varied from 10^{-3} down to 10^{-13} with an additional
194 error bound defined for the time iteration and having a value of 10^{-8} . The error bound
195 can be defined as the incremental limit between consecutive iterations of the algorithm
196 that produces a converged solution, thus determining the accuracy of the iterative
197 solutions. The accuracy of the iterative method has been evaluated in terms of accuracy
198 by comparing the difference in distance d between the iterated solution to the PD
199 location and the actual PD location. Four categories of location accuracy were defined:

- 200 • Very good accuracy: $d \leq 1$ cm
- 201 • Good accuracy: $1 \text{ cm} < d \leq 50$ cm
- 202 • Poor accuracy: $50 \text{ cm} < d \leq 1$ m
- 203 • Very poor accuracy: $d > 1$ m

204 Moreover, the computational efficiencies of the algorithms were assessed by calculating
205 the total number of iterations used to achieve converge on the stipulated error bound
206 accuracy. This was repeated for both antenna array configurations.

207 Regarding the non-iterative methods, these are well known for providing precise
208 estimates of the location when they are provided with accurate TDOAs [23]. In GPS,

209 there are always uncertainties in TDOA measurements and satellite positions. These
210 inaccuracies give rise to random errors of the emitter location. However, the location
211 accuracy can be improved by solving the clock error of the receiver [24], by using
212 pseudo-range observations [22] or by limiting the TOA range based on the altitude of
213 the GPS satellites [25].

214 Determining the location of PD using non-iterative methods is a more difficult process,
215 as PD sources do not provide a time of emission to establish synchronisation with the
216 receiving sensors. In this context, results sections of the non-iterative algorithms
217 evaluate the output of the two solutions provided by these algorithms as the simulated
218 PD have accurate theoretical TOAs based on equation (1). The accuracy of the non-
219 iterative algorithms have been evaluated in terms of PD location by determining the
220 difference between the calculated PD solutions (i.e. two roots solutions provided by the
221 quadratic equations of the algorithms) and the simulated positions. Two categories were
222 defined:

- 223 • Correct location: difference between calculated PD solution and simulated PD
224 position equal to 0.
- 225 • Incorrect location: difference between calculated PD solution and simulated PD
226 position not equal to 0.

227 **4 Location Performance of the Algorithms**

228 The following sections present the location results of the SLS and Bancroft algorithms
229 using the two different antenna arrangements. The location results will be discussed in
230 terms of location accuracy for both iterative and non-iterative methods and also the
231 number of iterations for the SLS algorithm.

232 4.1 Standard Least Squares (SLS) algorithm

233 4.1.1 Y-shaped array

234 To ensure converged solutions for all 64 simulated PD locations, sufficient iterations
235 were applied to the SLS algorithm for various error bounds. For the specified error
236 bounds, Figure 3 plots the number of converged PD location solutions within each of
237 the four accuracy categories defined above. It can be seen that the number of PD
238 sources located with very poor accuracy (greater than 1m from the simulated locations)
239 saw a marked decrease as the error bound reduced, allowing improvement in the
240 intermediate distances and convergence towards highly accurate positions (i.e 34
241 solutions less than 1 cm from the true PD source position). As the error bound was
242 reduced further, no additional improvement was seen. This result demonstrates that
243 location accuracy is influenced not only by the physical arrangement of the antennas,
244 the TDOA of the signals and the accuracy of the digital sampling hardware, but also on
245 the error bound set within the location algorithm.

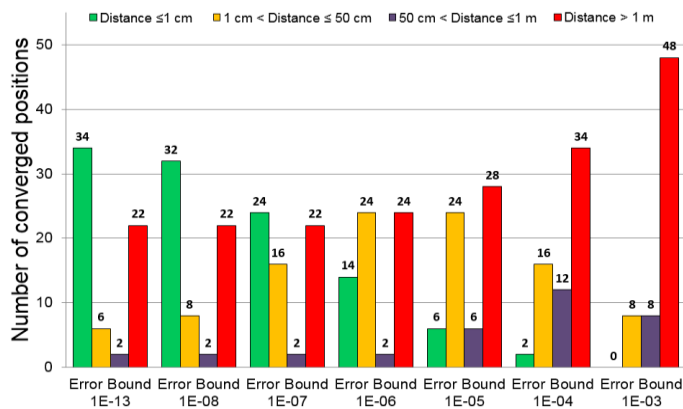


Figure 3: Number of converged PD position solutions as a function of location accuracy and error bound for simulations on the Y-shaped antenna array (SLS)

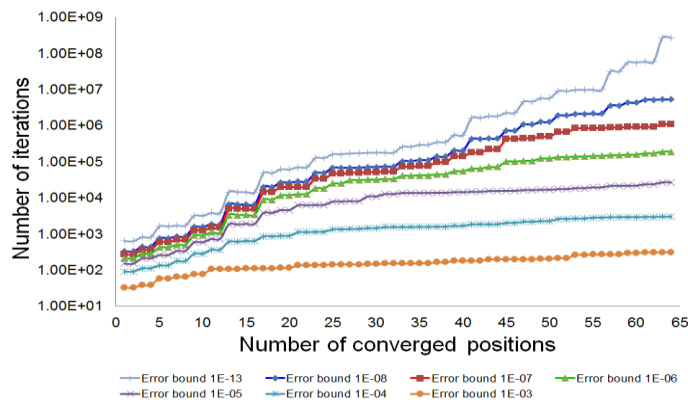


Figure 4: Results of simulations on the Y-shaped antenna array showing number of iterations vs. number of converged PD positions for various error bounds (SLS).

246 Figure 4 plots the total number of iterations needed for solutions to converge on all 64
 247 PD locations for the seven error bounds under consideration. This result demonstrates
 248 the relationship between the number of iterations and the error bound, with the former
 249 increasing significantly from a few hundred to hundreds of millions as the error bound
 250 decreases. Such a large number of iterations has the consequence of increasing
 251 computational time from a few seconds to several hours using a standard desktop
 252 machine (computation of these results were carried out using an Intel Q6600 Core2
 253 Quad 2.4 GHz Processor). Extended computing times would be impractical if location
 254 were required in real-time or close to real-time.

255 The percentage of PD sources pinpointed within the defined accuracy limits is shown in
 256 Table 2 together with the number of iterations performed for each respective error
 257 bound. It is clear from Table 2 that the location accuracy improves as the error bound
 258 decreases. Consequently, the iterative steps accumulate in number. Additionally, using
 259 the lowest error bound i.e. 10^{-13} , which was found to be the best possible accuracy for
 260 this arrangement, the number of PDs located at more than 1 m from the simulated
 261 positions was found to be slightly high. This is due to the spatial separation between the
 262 different antennas and the antenna arrangement as further results using the square
 263 antenna arrangement shows improved location accuracy.

Table 2: Results of SLS algorithm showing percentage of solutions converging within the defined location accuracy limits for the Y-shaped antenna array.

Error Bound	$d \leq 1 \text{ cm}$	$1 \text{ cm} < d \leq 50 \text{ cm}$	$50 \text{ cm} < d \leq 1 \text{ m}$	$d > 1 \text{ m}$	No. of Iterations
10^{-13}	53.1%	9.4%	3.1%	34.4%	275740268
10^{-08}	50.0%	12.5%	3.1%	34.4%	5371396
10^{-07}	37.5%	25%	3.1%	34.4%	1104646
10^{-06}	21.9%	37.5%	3.1%	37.5%	194065
10^{-05}	9.4%	37.5%	9.4%	43.8%	27325
10^{-04}	3.1%	25%	18.8%	53.1%	3164
10^{-03}	0.0%	12.5%	12.5%	75.0%	315

Table 3: Results of SLS algorithm showing percentage of solutions converging within the defined location accuracy limits for the square-shaped antenna array.

Error Bound	$d \leq 1 \text{ cm}$	$1 \text{ cm} < d \leq 50 \text{ cm}$	$50 \text{ cm} < d \leq 1 \text{ m}$	$d > 1 \text{ m}$	No. of Iterations
10^{-13}	95.3%	0%	0%	4.7%	2212354990
10^{-08}	84.4%	10.9%	0%	4.7%	11755016
10^{-07}	67.2%	26.6%	1.6%	4.7%	1727533
10^{-06}	29.7%	57.8%	6.3%	6.3%	243296
10^{-05}	7.8%	60.9%	15.6%	15.6%	55905
10^{-04}	1.6%	34.4%	15.6%	48.4%	4140
10^{-03}	0%	18.8%	15.6%	65.5%	263

264 4.1.2 Square-shaped array

265 The results obtained using SLS with the square antenna array proved similar to those
266 obtained previously with regards to the accuracy and number of iterations (See Figure 5
267 and Figure 6). With an error bound of 10^{-03} , 42 PD positions were located with very
268 poor accuracy (metres from their true position). The number of PD located $> 1 \text{ m}$ from
269 the simulated positions was reduced significantly as the error bound became smaller,
270 allowing the intermediate distances to improve and solutions to converge towards very
271 accurate locations of less than 1 cm from the true PD source position. However, Table 3
272 shows a considerable improvement of the location accuracy. At an error bound of 10^{-13} ,
273 95.3% of iterated PD positions were to within an accuracy of less than 1 cm. Whereas,
274 in the case of the Y-shaped array configuration, only 53.1% of PD were located to
275 within the same accuracy at the same error bound. The 3 remaining PD positions

276 located at a distance of > 1 m did not show any further improvement despite further
 277 reduction in the error bound. The non-location of these PD positions was mainly due to
 278 the applied initial value $(0, 0, 0)$ since, after replacing those initial values by the actual
 279 true value of the PD locations, calculation provided a correct solution.

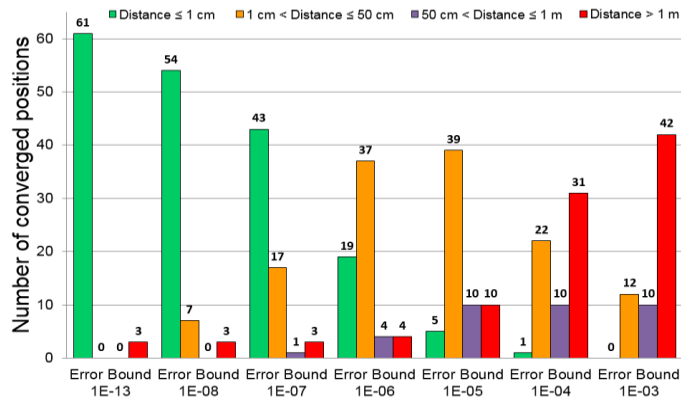


Figure 5: Number of converged positions as a function of both location accuracy and error bound for square shaped arrangement (SLS)

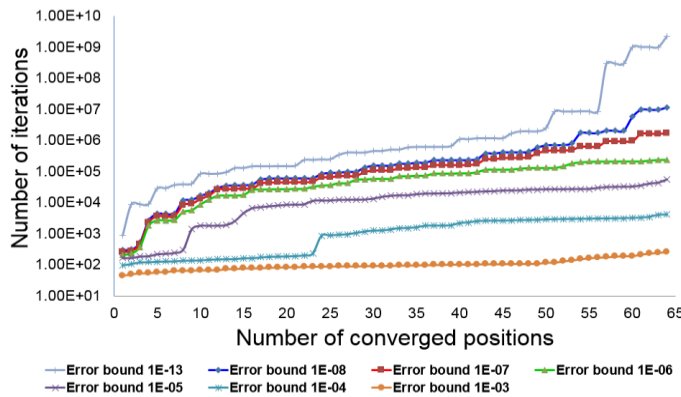


Figure 6: Results of simulations on the square-shaped antenna array showing number of iterations vs. number of converged PD positions for various error bounds (SLS).

280 4.1.3 Discussion

281 As shown in Table 2 and Table 3, which present respectively the effectiveness of the Y
 282 and square shape arrays to locate PD occurring at each of the 64 grid positions, it can be
 283 seen that in the case of the square array, 95.3% of the converged solutions locate PD to
 284 within 1 cm of their true position at an error bound of 10^{-13} . In contrast, the Y shaped

285 array, is only capable of locating 53.1% of the PDs to within than 1 cm of their true
 286 position at the same error bound, which represents the best possible accuracy for this
 287 arrangement in the present study. These results show that in addition to the influence of
 288 the algorithms' error bound and the number of iteration on the location accuracy,
 289 antenna arrangement are also key for enhanced location results. This is mostly due to
 290 the square antenna arrangement having a better spatial separation and better coverage
 291 area than the Y shaped antenna arrangement.

292 In Figure 7 which shows the number of PD positions located with an accuracy of 1 cm
 293 or less as a function of error bound, one may conclude that, while requiring more
 294 iterations, the SLS algorithm as applied to PD location using the square array, generally
 295 produces more accurate results than with the Y shaped array (see Figure 8).

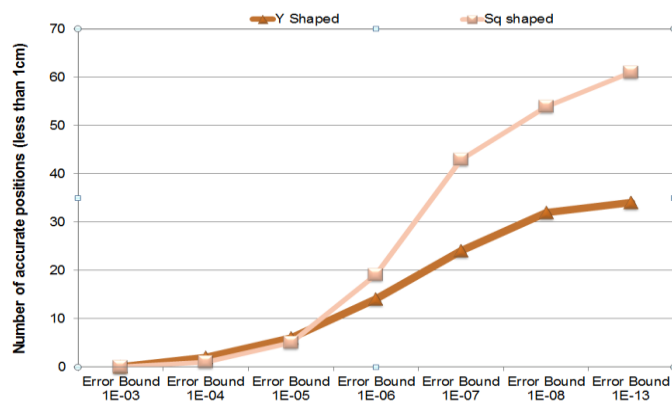


Figure 7: Number of accurate PD location solutions (< 1 cm from the PD source) for the two array configurations as a function of error bound (SLS)

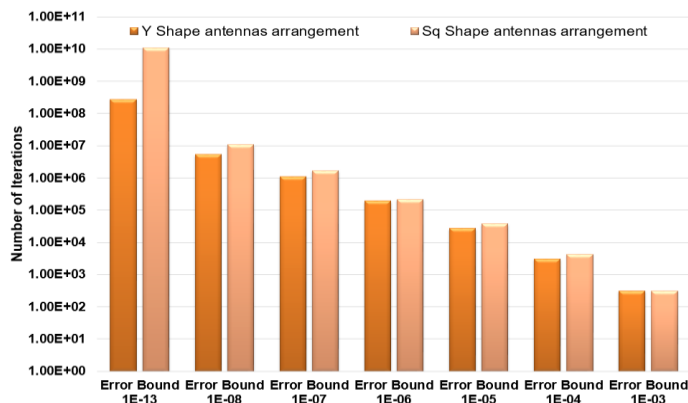


Figure 8: Number of iterations required to achieve converged solutions for each antenna configuration as a function of error bound (SLS)

296 **4.2 Bancroft algorithm**

297 Bancroft [21] determined a closed form expression for global positioning system
298 pseudo-range equations. In his derivation of the formula, Bancroft made use of the
299 Lorentz inner product and demonstrated that pseudo-range equations are hyperbolic in
300 nature and may have two solutions. Although he did explicitly discuss the GPS
301 navigation solution which determines the coordinates (x, y, z) and the clock offset of a
302 GPS receiver, the understanding of the two solutions provided by the algorithm with
303 regard to partial discharge location using RF technique is investigated in the following
304 paragraphs.

305 **4.2.1 Y shaped antenna array**

306 To evaluate the performance of the two solutions provided by the Bancroft algorithm,
307 the 64 PD positions defined on the simulation grid were computed by the Bancroft
308 algorithm as described in Section 3. Figure 9 presents the number of correct and
309 incorrect location solutions provided by both the positive and negative root.

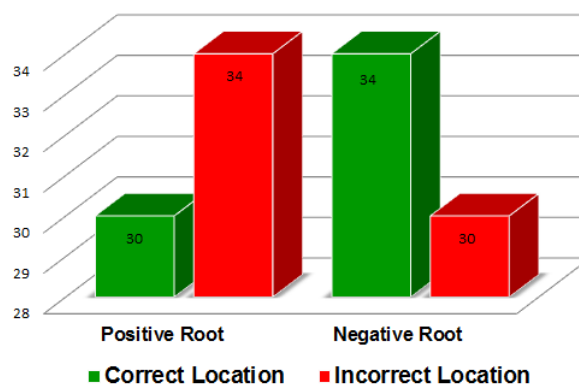


Figure 9: Location results of Bancroft algorithm using Y shaped antenna arrangement

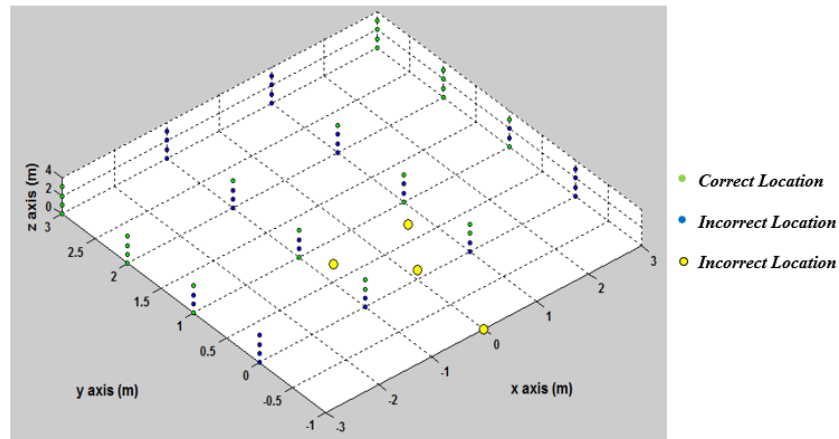


Figure 10: Position of located and non-located PD using Y shaped antenna arrangement and positive root of the Bancroft algorithm

310 Based on results of the positive root of the Bancroft algorithm, it can be seen that the
 311 algorithm provided accurate positioning to 30 PD locations and 34 incorrect solutions to
 312 the remaining PD positions. This demonstrates that the algorithm can only provide
 313 partial results to the 64 simulated PD using one of the roots and that the location of
 314 these simulated PD require the investigation of both solutions.

315 The exact position of the located and non-located PD is presented in Figure 10, where
 316 the green points represent the located positions and the blue points the incorrect
 317 solutions. It can be seen from the figure that the positioning results of located and non-
 318 located PD positions are symmetrical around the antenna central point. This is due to
 319 the topology of the Y shaped array, of which the y and z coordinates of antennas 3 and 4
 320 are identical.

321 Regarding the location results of the Bancroft algorithm using the negative root, it can
 322 be seen from Figure 9 that the algorithm provided 34 accurate PD locations and 30
 323 inaccurate PD locations. It should be noted that inaccurate locations using the positive
 324 root are found to be located accurately using the negative root and vice versa. This
 325 demonstrates that the algorithm can provide accurate locations to the 64 simulated PD

326 positions if valid solutions are selected between both roots. This demonstrates that the 2
327 solutions provided by the algorithm complement each other to provide accurate
328 positioning to the simulated PD. This is because the two hyperbolas intersect at two
329 locations, one that corresponds to the TDOA with correct sign and the other to the
330 TDOA with reversed sign.

331 4.2.2 Square shaped antenna arrangement

332 Using the square antenna arrangement and the positive root, the Bancroft algorithm
333 provided 17 correct locations and 47 incorrect locations (see Figure 11). On the other
334 hand, positioning results using the negative root provided more accurate locations than
335 the positive root, where 52 out of the 64 simulated PD positions located accurately and
336 only 12 PD were located incorrectly. The difference between the correct PD locations
337 using the positive root and the non-located PD using the negative root results from 5 PD
338 positions being located accurately by both roots.

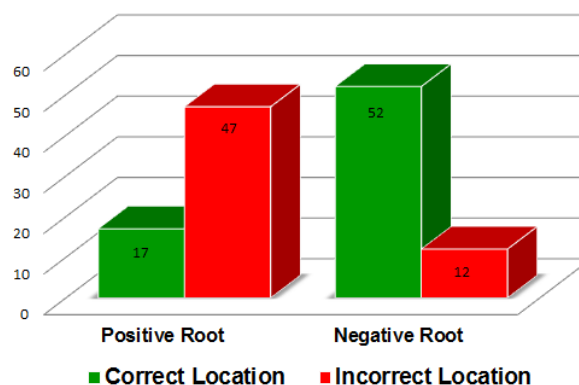


Figure 11: Location results of Bancroft algorithm using square shaped antenna arrangement

339 4.2.3 Discussion

340 Based on the results of the Bancroft algorithm using both positive and negative roots, it
341 can be seen that the algorithm can provide very accurate location results on the 64
342 simulated PD positions. Results also show that the algorithm provided more successful
343 location results when using the negative root instead of the positive root. In addition,

344 location results using the square antenna arrangement were found to be better than the
345 location results when using the Y shaped antenna arrangement. Although location
346 results using the different antenna arrangements differ in terms of the number of
347 successfully located PD using each root, the discrimination between correct and
348 incorrect solutions of the positive and negative root can be carried out using the clock
349 offset parameter. Based on the simulated PD, it was found that the Bancroft algorithm
350 can provide 100% accurate solutions to the simulated PD positions when selecting the
351 cartesian coordinates (x, y, z) corresponding to the lowest clock offset when comparing
352 results of both roots. Validation of this selection process may change when considering
353 noise effects and measurement errors as time offset adjustments cannot be established
354 due to the stochastic nature of the physical PD emission process.

355 Additionally, given only the difference in arrival times of the antennas' signals, it is
356 difficult to know which solution is correct. The separation between the algorithm's
357 correct and incorrect solutions will depend on the environment where measurements
358 took place. For example, in the case where measurements are carried out in a high
359 voltage power transformer using acoustic sensors attached to the transformer's housing,
360 discrimination between the different solutions can use the equipment's area spatial
361 volume to limit the search of valid solutions. In the case of open space areas such as
362 electrical substations, if the reference point is at the ground height and the locations of
363 interest are in front of the antenna arrangements, one can limit the search of valid
364 solutions within the positive interval of y and z coordinates.

365 **5 Comparison between Iterative and Non-Iterative Algorithms**

366 Nonlinear equations of location algorithms which are presented by hyperbolas and
367 distance formulas are commonly solved with iterative algorithms [26]. Results of the
368 iterative algorithm showed that these methods have strong dependencies on different

369 parameters such as the error bound, number of iterations and also initial values which
 370 must be provided by the user. On the other hand, non-iterative methods, which do not
 371 require iterations and therefore make a fast computation tool, showed that they provide
 372 very accurate location results when provided by accurate TDOAs (in this case,
 373 theoretical TDOAs were provided). However the selection of correct locations among
 374 the two available solutions will depend on the user's experience and ability to
 375 discriminate between the different positioning solutions by using for example time
 376 restrictions based on the equipment's spatial volume. Table 4 presents some of the
 377 advantages and disadvantages of the different location algorithms when applied to PD
 378 location.

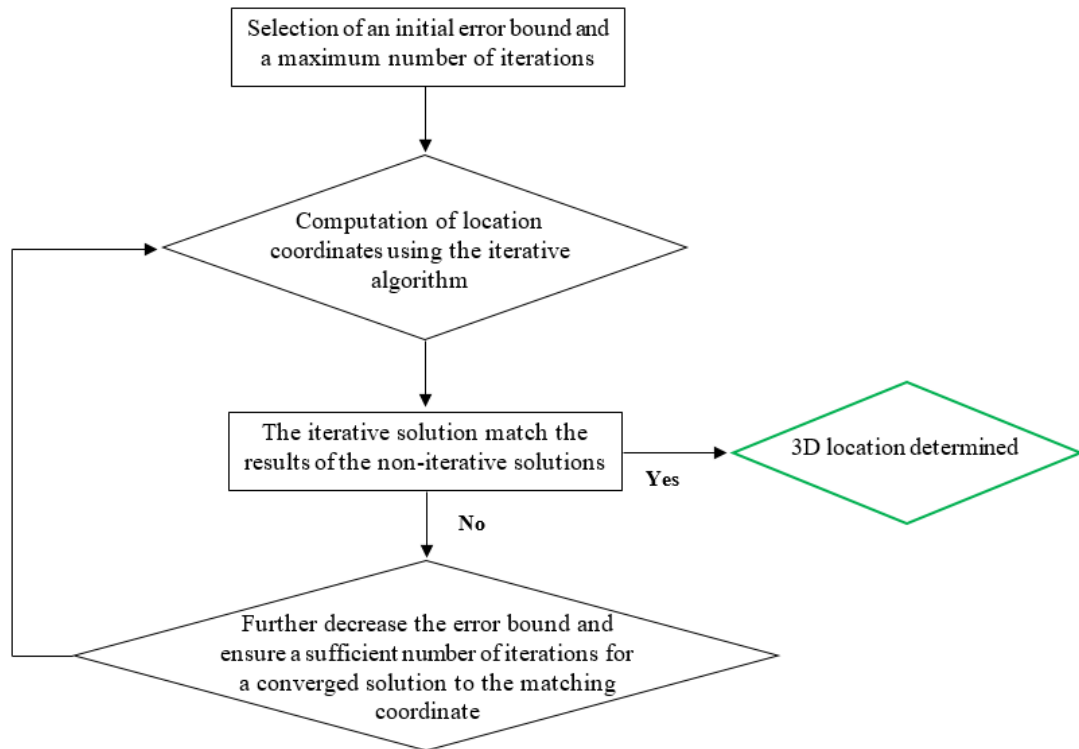
Table 4: Characteristics of the location algorithms

Algorithm	Advantages	Disadvantages
Iterative (SLS)	<ul style="list-style-type: none"> • Accurate if provided with well selected error bound • Accurate if provided with well selected number of iterations • Accurate if provided with accurate time of arrival 	<ul style="list-style-type: none"> • Depends on number of iterations • Depends on error bound • Depends on initial values • Depends on antenna arrangement
Non-Iterative (Bancroft)	<ul style="list-style-type: none"> • Direct solution • Fast and very accurate • Do not depend on initial values • Possibility of discriminating between the two solutions (Bancroft method only) 	<ul style="list-style-type: none"> • No indication of converged solutions • Depends on time of arrival accuracy • No way of discriminating between the two solutions • Provide two different solutions • Depends on antennas arrangement

379 Using iterative methods, the question which is still raised is: how can the user define a
 380 valid error bound and also a valid number of iterations sufficient to provide accurate
 381 location results assuming there is no initial values issue (see example of SLS
 382 performance at 10^{-13} error bound in Figure 5)?

383 **6 New Approach**

384 Based on simulations, it was found that when the error bound is high (e.g. 10^{-3} error
385 bound), solutions of the location coordinates are often underestimated and the number
386 of iterations required is also low. When the location coordinates of some TDOAs using
387 the iterative results are compared to the location coordinates of the same TDOAs using
388 non-iterative methods, this may show a location mismatch in the case of a non-valid
389 error bound selection and which indicates that the error bound should be decreased.
390 This process should be repeated until matching results are found by both iterative and
391 non-iterative methods. Regarding the selection of a valid number of iterations, this is
392 determined by providing enough iteration values which allow a converged solution
393 based on the matching solutions of both iterative and non-iterative methods to be
394 obtained. Figure 12 summarises the selection process of valid error bounds and number
395 of iterations used by the iterative methods based on the non-iterative method solutions.
396 It should be noted that the iterative methods may sometimes provide a non-converged
397 solutions which may be due to initial values issue or measurement errors.



398

399

Figure 12: Selection of error bound and number of iterations

400 7 Conclusions

401 As a study evaluating the location accuracy of an iterative and non-iterative algorithms

402 as applied to partial discharge measurement, simulations of a range of PD using two

403 different antenna configurations have been presented.

404 By varying the error bounds, it has been shown that the performance of the iterative

405 algorithms as a function of location accuracy can be quantified, despite the nonlinear

406 nature of the location equations. A decrease in the error bound produces more accurate

407 location results while requiring more iterations. The results presented will be useful for

408 a practitioner of condition monitoring of in-service power equipment since it will allow

409 judgement of appropriate levels of required accuracy based on the dimensions of the

410 equipment under surveillance. It will also facilitate estimation of the required

411 computing time to achieve the desired level of location accuracy. The required spatial

412 location accuracy depends on the application. For example, general surveying of

413 equipment on a substation-wide scale may only require a poor to good level of accuracy
414 ($1 \text{ cm} \leq d \leq 1 \text{ m}$). This range may also accurately facilitate the location of faults along
415 large equipment sections such as busbars, bushings or power transformers (i.e. larger
416 equipment).

417 Regarding the non-iterative algorithms, it was found that these techniques provide very
418 accurate positioning when provided with precise TDOAs. The accuracy of the non-
419 iterative algorithms also depends on the antenna arrangements which influence the
420 number of accurate positions located by the two different roots. The discrimination
421 process between the two different solutions of the non-iterative solutions can be
422 difficult and will depend on the user experience to separate between the two solutions
423 using, for example, time restrictions based on the equipment's spatial volume.

424 A novel approach to select adequate error bounds and number of iterations using results
425 of the non-iterative methods has been established and will contribute considerably to
426 solve some of the iterative method dependencies.

427 In this work, simulations provided an evaluation of the performance of different types
428 of location algorithms based on determined PD locations. This evaluation method gives
429 indications of the essential characteristics of iterative methods and also an insight on the
430 behaviour of non-iterative methods to provide different solutions. The study presented
431 in this paper can benefit electrical utilities, network operators and designers of PD
432 locations systems, as it can be used as a guide to the selection of specific algorithm
433 based on its operation requirements (i.e. computation time, discrimination between
434 solutions, accuracy parameters and their selection process), facilitating more accurate
435 location and diagnosis of incipient faults in high value electrical power equipment.

436 **Acknowledgements**

437 The work presented in this paper were obtained as part of a financial, academic and
438 technical support provided by Glasgow Caledonian University during the main author
439 PhD studies.

440 **References**

- 441 [1] Moore, P. J., Portugues, I. E., and Glover, I. A. "Radiometric location of partial
442 discharge sources on energized high-voltage plant" IEEE Transactions on Power
443 Delivery, 2005, 20, (3), pp 2264-2272
- 444 [2] Stewart, B. G., Nesbitt, A., and Hall, L. "Triangulation and 3D location
445 estimation of RFI and partial discharge sources within a 400kV substation"
446 Proceedings on IEEE Electrical Insulation Conference, Montreal, Canada , June
447 2009, pp 164-168
- 448 [3] Tian, Y., Kawada, M., and Isaka, K. "Locating partial discharge source
449 occurring on distribution line by using FDTD and TDOA methods" IEEE
450 Transactions on Fundamentals and Materials, 2009, 129, (2), pp 89-96
- 451 [4] El Mountassir, O. Stewart, B, G. McMeekin, S. G. and Ahmadinia, A.
452 "Evaluation of an iterative method used for partial discharge RF location
453 techniques", 10th International Conference on Environment and Electrical
454 Engineering, 2011, pp 1-4
- 455 [5] Coenen, S. and Tenbohlen, S. "Location of PD sources in power transformers by
456 UHF and acoustic measurements" IEEE Transactions on Dielectrics and
457 Electrical Insulation, 2012, 19, pp 1934-1940
- 458 [6] Steiner, J. P., Reynolds, P. H., and Weeks, W. L. "Estimating the location of
459 partial discharges in cables" IEEE Transactions on Electrical Insulation, 1992,
460 27, pp 44-59
- 461 [7] Tian, Y., Lewin, P., Davies, A., Sutton, S., and Swingler, S. "Partial discharge
462 detection in cables using VHF capacitive couplers" IEEE Transactions on
463 Dielectrics and Electrical Insulation, 2003, (10), pp 343-353

- 464 [8] Mardiana, R. and Su, C. Q. "Partial discharge location in power cables using a
465 phase difference method" IEEE Transactions on Dielectrics and Electrical
466 Insulation, 2010, (17), pp 1738-1746
- 467 [9] Wagenaars, P., Wouters, P. A. A. F., Van der Wielen, P. C. J. M., and Steennis,
468 F. "Influence of ring main units and substations on online partial discharge
469 detection and location in medium voltage cable networks" IEEE Transactions on
470 Power Delivery, 2011, (26), pp 1064-1071
- 471 [10] Meijer, S., Smit, J. J. and Girodet, A. "Estimation of UHF signal propagation
472 through GIS for sensitive PD detection" IEEE International Symposium on
473 Electrical Insulation, 2002, pp 435-438
- 474 [11] Hu, X., Judd, M. D., and Siew, W. H. "A study of PD location issues in GIS
475 using FDTD simulation". International Universities Power Engineering
476 Conference, 2010, pp 1-5
- 477 [12] Hikita, M., Ohtsuka, S., Wada, J., Okabe, S., Hoshino, T., and Maruyama, S.
478 "Study of partial discharge radiated electromagnetic wave propagation
479 characteristics in an actual 154kV model GIS" IEEE Transactions on Dielectrics
480 and Electrical Insulation, 2012, (19), pp 8-17
- 481 [13] Chiu, M. Y., Liang, K.W., Lee, C. H., Fan, C. L., Cheng, J., and C., L. Y.
482 "Application of MV GIS partial discharge measurement and location"
483 International Conference on Condition Monitoring and Diagnosis, 2012, pp 462-
484 465
- 485 [14] Zheng, B and Bojovschi, A. "Electromagnetic Sensing of Partial Discharge in
486 Air-insulated Medium Voltage Switchgear", IEEE Power Engineering and
487 Automation Conference, 2012, pp 1-4

- 488 [15] Judd, M. D., Yang, L., and Hunter, I. B. B. "Partial discharge monitoring for
489 power transformer using UHF sensors. Part 2: Field experience" IEEE Electrical
490 Insulation Magazine, 2005, (21), pp 5-13
- 491 [16] Tang, Z. G., Chengrong, L. R., Xu, C. ; Wei, W., Jinzhong, L., and Jun, L.
492 "Partial discharge location in power transformers using wideband RF detection"
493 IEEE Transactions on Dielectrics and Electrical Insulation, 2006, (13), pp 1193-
494 1199
- 495 [17] Sinaga, H. H., Phung, B. T., and Blackburn, T. R. "Partial discharge localization
496 in transformers using UHF detection method" IEEE Transactions on Dielectrics
497 and Electrical Insulation, 2012, (19), pp 1891-1900
- 498 [18] Zhang, X., Tang, J., and Xie, Y. "Taylor-genetic algorithm on PD location"
499 International Conference on High Voltage Engineering and Application, 2008,
500 pp 685-688
- 501 [19] Miao, P., Li, X., Huijuan, H., Gehao, S., Hu, Y., and Jiang, X. "Location
502 algorithm for partial discharge based on radio frequency (RF) antenna array"
503 Asia-Pacific Power and Energy Engineering Conference, 2012, pp 1-4
- 504 [20] Y. Lu, X. Tan, X. Hu, "PD detection and localisation by acoustic measurements
505 in an oil-filled transformer", IEEE Transactions on Science, Measurement and
506 Technology, 2002, (147), pp 81-85
- 507 [21] O. El Mountassir, B. G. Stewart, S. G. McMeekin and A. Ahmadinia. "Effect of
508 sampling rate on the location accuracy of measurements from radiated RF partial
509 discharges signals" 11th International Conference on Environment and Electrical
510 Engineering, 2011, pp 891-896
- 511 [22] Bancroft, S. "An algebraic solution of the GPS equations" IEEE Transactions on
512 Aerospace and Electronic Systems, 1985, (21), pp 56-59

- 513 [23] Ho, K. M. and Chan, Y. T. "Solution and performance analysis of geolocation
514 by TDOA" IEEE Transactions on Aerospace and Electronic Systems, 1993,
515 (29), pp 1311-1322
- 516 [24] Yang, M. and Chen, K. H. "Performance assessment of a noniterative algorithm
517 for global positioning system (GPS) absolute positioning" Proceedings of the
518 National Science Council, 2001, (25), pp 102-106
- 519 [25] Bucher, R. and Misra, D. "A synthesizable VHDL model of the exact solution
520 for three-dimensional hyperbolic positioning system" VLSI Design Journal,
521 2002, (15), pp 507-520
- 522 [26] Markalous, S., Tenbohlen, S., and Feser, K. "Detection and location of partial
523 discharges in power transformers using acoustic and electromagnetic signals"
524 IEEE Transactions on Dielectrics and Electrical Insulation, 2008, (15), pp 1576-
525 1583

Research Highlights

- The location performance of an iterative and non-iterative algorithms is proposed
- Iterative methods depend on error bound, number of iterations and antenna array
- Decrease of the error bound results in increased location accuracy and iterations
- Non-iterative methods provide accurate location results if the TDOAs are accurate

Response to Reviewers

Quantification of the Performance of Iterative and Non-Iterative Computational Methods of Locating Partial Discharges Using RF Measurement Techniques	
Reviewer #1	
Comments	Responses
No additional comments	
Reviewer #2	
The reviewer has accepted the paper in the last revision. Non additional changes are requested	
Reviewer #3	
Editorial comments	
1	Line 90: do not write the unit in italic
2	Line 95: indices should not be in italic, except they are variables
3	Line 96: n is a variable and should be written in italic n
4	Figure 2: quality of Fig. 2 is not good and could be improved
5	Table 3: place the table on one side
6	Fig. 8: legend is difficult to read; use different colors for the type of antennas
7	Fig. 12: quality of Fig. 12 is not good and could be improved
All edits and changes to figures were addressed as per by the reviewer recommendations.	
Technical Comments	
1	Equ.13: What is s in this equation?
s is the location of interest and is defined in equation 10. To avoid confusion, the definition of all the parameters of equation 13 now includes variable "s".	

Offshore Renewable Energy Catapult
121 George Street
Glasgow
G1 1RD
UK

11th October 2016

Dear Editor,

Please find attached a revised copy of the manuscript entitled "Quantification of the Performance of Iterative and Non-Iterative Computational Methods of Locating Partial Discharges Using RF Measurement Techniques". This manuscript is submitted for consideration for publication as an original research paper within the Electric Power Systems Research.

We hereby confirm that this manuscript is our original work, has not been published previously and it is not being reviewed for publication by another organisation.

Yours faithfully,

Dr Othmane El Mountassir
Project Engineer

Telephone: (+44) 3330 041 346
E-mail: othmanee.el.mountassir@ore.catapult.org.uk